OPERATIONAL PREDICTION AND SPECIFICATION OF THE SPACECRAFT CHARGING ENVIRONMENT

Terrance Onsager
National Oceanic and Atmospheric Adminstration (NOAA)
NOAA Space Environment Center
325 Broadway
Boulder, CO 80305
Phone: 303-497-5713
E-mail: terry.onsager@noaa.gov

Introduction

Fluxes of outer radiation belt electrons change dramatically over a broad range of time scales, ultimately driven by the solar wind, but controlled within the magnetosphere by the action of numerous acceleration and loss mechanisms. The particle dynamics are influenced by both adiabatic and non-adiabatic processes, involving in-situ acceleration or loss as well as diffusion either into or out of the radiation belt across its inner and outer boundaries. (see recent review by Friedel et al. [2002]). Although many different processes have been shown to cause either acceleration or loss of radiation belt particles under different circumstances, there currently is not a quantitative understanding of which processes dominate under any specific conditions. Without this quantitative understanding of the competing source and loss mechanisms, accurate physics-based modeling of the time-dependent radiation belts is not possible.

The processes that either accelerate or deplete the radiation belt electrons do not operate uniformly throughout the magnetosphere, and therefore gradients will develop in the radial distribution of electrons. These gradients could be created, for example, through enhanced wave energization or scattering into the loss cone within the radiation belts in the inner magnetosphere [e.g. Horne and Thorne, 1998; Elkington et al., 2003], or through increases or decreases in the electron phase space density in the outer magnetosphere, at the outer boundary of the trapped radiation belts [e.g., Brautigam and Albert, 2000]. Radial diffusion, which is a primary mechanism for radial transport, will then act to reduce the gradient, transporting plasma from locations of high phase space density to low. Because the various source and loss processes may operate at different times and locations within or outside the radiation belts, the continuous measurement of the radial profile of phase space density is one important way of identifying which processes are acting at which times.

One of the most significant impediments to identifying peaks or gradients in phase space density is that our in-situ satellite measurements are not available in terms of the adiabatic invariants. When expressed in terms of parameters other than the adiabatic invariants, such as fixed energy, the electron flux can undergo huge variability due entirely to adiabatic (i.e., reversible) processes [e.g., Li et al., 1997; Kim and Chan, 1997]. Only when the adiabatic behavior of the electrons is known can the important non-adiabatic source and loss processes be quantified and understood. From knowledge of phase space density in terms of the adiabatic invariants, key quantities for understanding radiation belt dynamics, such as its radial gradient, can be calculated and analyzed.

Although we have extensive data sets acquired by a large number of satellites over decades, no long-term characterization of the radiation belts in terms of adiabatic invariants exists today. Calculations of phase space density in terms of adiabatic invariants have been done on short, isolated intervals of data, in most cases concentrating on dynamic geomagnetic storm intervals [Selesnick and Blake, 1997a; 1997b; 1998; 2000; Hilmer et al., 2000; McAdams et al., 2001]. Estimates of the radial gradient of phase space density have been made in two ways. One technique has been to use satellites whose orbits cross a large range of L-shells, such as CRRES and Polar, to calculate phase space density for fixed values of the first two adiabatic invariants over individual orbits or consecutive orbits [e.g., Brautigam and Albert, 2000; Selesnick and Blake, 2000]. The other technique utilizes simultaneous measurements from satellites widely separated in radial distance, such as GPS measurements at L = 4.2 and geosynchronous measurements at L = 6.6 to estimate the radial profile of phase space density [e.g., Hilmer et al., 2000; McAdams et al., 2001].

The CRRES and Polar results suggest that a peak in phase space density occurs inside geosynchronous orbit associated with radiation belt enhancements, but that phase space density generally increases with increasing radial distance from inside to outside geosynchronous orbit during quiet times. Through the GPS and LANL comparisons, phase space density has been consistently found to be higher at L = 6.6 than at L = 4.2; however, measurement of the local gradient at geosynchronous orbit or additional observations inside or outside geosynchronous orbit would be required to further constrain the location of the peak. These studies have also highlighted the large uncertainty in calculations of phase space density in terms of adiabatic invariants, and the ambiguity of the location of its peak due to uncertainties in the global field model and the details of the electron distribution function.

The focus of this effort will be to develop a new technique for determining the radial gradient of phase space density at geostationary orbit, and to apply this technique under a wide variety of solar wind and geomagnetic conditions. The primary data we will use are from the GOES 8, 9, 10, 11, and 12 satellites, which measure energetic particle flux and magnetic field. Although the GOES satellites are three-axis stabilized while in operational use, a number of the GOES satellites acquired data while spinning during on-orbit storage. Data from the spinning satellites allow us to calculate electron pitch angle distributions, which are key to accurately estimating phase space density. These data are available over years of geosynchronous measurements, allowing us also to characterize the pitch angle distributions as a function of local time and geomagnetic activity. These data will be augmented during selected time periods with data from the LANL geosynchronous satellites and from the POLAR satellite to further constrain the global magnetic field and to provide valuable inter-calibration of flux levels, energy spectra, and pitch angle information obtained from the different instruments to more accurately determine phase space density and its gradient.

Our research will answer the following questions: What is the radial gradient of phase space density at geosynchronous orbit? How does the direction of the gradient vary from quiet to active times? How does the direction of the gradient vary between key phases of the solar cycle, such as during storms driven by solar wind transients versus radiation belt enhancements driven by high-speed streams? How sensitive is the calculation of phase space density in adiabatic invariant space to uncertainties in the electron pitch angle distribution, energy spectrum, and to

inaccuracies in the global magnetic field models? How do the electron pitch angle distributions vary with local time, geomagnetic activity, and magnetic field inclination?

In addition to determining the local gradient of phase space density, we will provide a long-term reference for phase space density in terms of adiabatic invariants at multiple locations in geostationary orbit over years of data that can be used by other researchers for comparison with data from other satellites. We will make the databases of phase space density mapped to adiabatic-invariant space and our computer codes available to the research community. The database will include the raw measurements of integral flux, magnetic field, and the calculated phase space density mapped to adiabatic invariant space. The computer codes will enable the calculation of the adiabatic invariants (*M, K*, and *L**) using a set of publicly available magnetic field models.

The results of this research will have direct relevance to four of the five NASA Strategic Enterprises. This research will quantify the dynamics of an important aspect of the Sun-Earth system over a large fraction of a solar cycle (a goal of the Space Science Enterprise), and improve our understanding of the radiation environment that is important both for human activities in space (Biological and Physical Research Enterprise and Human Exploration and Development of Space Enterprise) and for space system design (Aerospace Technology Enterprise). This research will provide critical new information on the location of the source and loss processes affecting the radiation belt electrons, and therefore contribute directly to our ability to predict changes in Earth's radiation belt environment through internal processes and through solar wind driving, which is directly relevant to Strategic Goal 1, Sun-Earth Connection Theme, RFA 1(b) and Strategic Goal 2, Sun-Earth Connection Theme, RFA 1(c). From the error analyses we conduct, we will help to define the requirements for future Living With a Star missions, such as the Radiation Belt Storm Probe mission.

Calculating Phase Space Density and its Radial Gradient

The GOES data provide the opportunity to calculate radiation belt electron phase space density in adiabatic-invariant space at multiple locations in geostationary orbit over a solar cycle. However, as mentioned above, there are numerous difficulties associated with making these calculations. In the following example, we describe the technique we will use to make these calculations, and we illustrate the sensitivity of our results to uncertainties in the energy spectrum and the pitch angle distributions. A potentially important source of error is introduced by the necessity of using a magnetic field model to characterize the global azimuthal drift of the electrons. For the example given here, we have chosen to analyze a geomagnetically quiet time, when the magnetic field models are likely to be the most accurate. An important part of this research will be to investigate in detail the consistency of simultaneous phase space density calculations at a large number of local times (using GOES and LANL geosynchronous satellites and Polar during crossings of the equatorial plane near geosynchronous orbit) during active as well as quiet times, and to determine if the agreement can be improved by utilizing the most recent magnetic field models that include azimuthal variations in the field.

A key application of our calculations of phase space density will be to determine its local radial gradient at geosynchronous orbit. As demonstrated below, the east and west GOES

satellites are located at different geomagnetic latitudes due to the tilt of Earth's dipole magnetic field. Therefore, these spacecraft provide simultaneous measurements in different *L*-shells. If phase space density and the adiabatic invariants can be determined with sufficient accuracy, these calculations will give a continuous measure of the local radial gradient of phase space density. Quantifying the accuracy of these calculations is an important part of this research. In addition, these calculations will give a valuable reference value for phase space density at geostationary orbit to allow comparison with other spacecraft in more largely separated *L*-shells, either inside geosynchronous orbit, such as GPS, or outside, such as POLAR or CLUSTER.

For the example we describe here, measurements of the GOES >2 MeV electron flux at geostationary orbit and Dst index on February 1-8, 1996 are shown in Figure 1. The top panel contains the electron flux at GOES-8 (solid) and GOES-9 (dashed), and the bottom panel contains the Dst index, courtesy of the World Data Center, Kyoto, Japan.

The electron flux was moderately high, with some periods of relatively little variability (Feb. 3-6) and some instances of fairly abrupt changes in the flux levels (e.g., Feb. 2 and Feb. 7), with no significant activity seen in Dst. An obvious feature of the electron flux at geostationary orbit is the consistent diurnal variation, with higher fluxes observed near noon and lower fluxes observed near midnight. This variation in the fluxes is due to the local-time asymmetry of the magnetic field and the fact that in the outer magnetosphere, particle flux at constant energy decreases with increasing distance from Earth. Other noticeable features in the electron data are that the fluxes measured by GOES 9 (dashed curve) appear to be offset in time relative to GOES 8 and have consistently higher values.

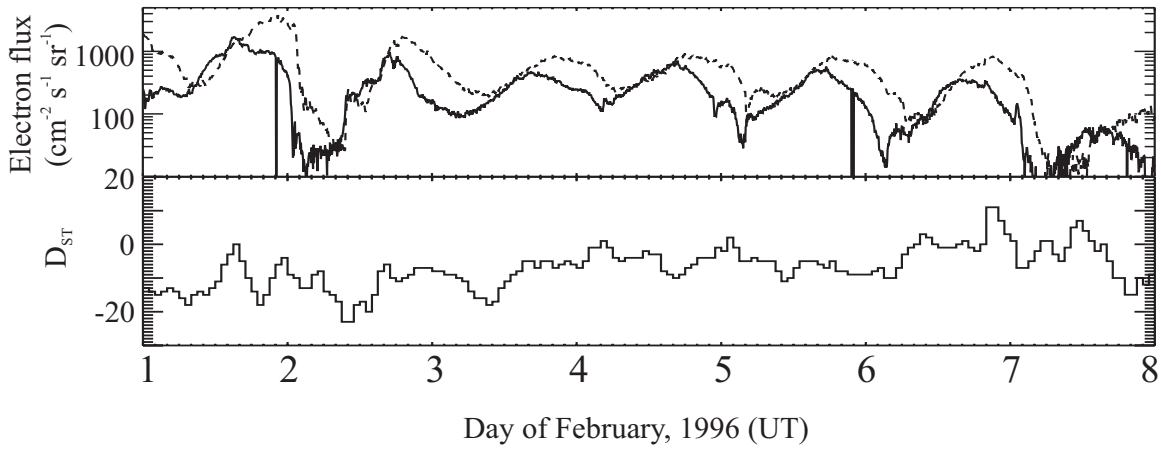

Figure 1. (Top) geosynchronous electron flux, and (bottom) Dst during an extended period with elevated >2 MeV electron flux and quiet geomagnetic conditions.

The difference in flux levels at the two spacecraft is due to the different longitudinal locations of the two spacecraft. Diagrams illustrating the locations of GOES 8 and 9 are shown in Figure 2. The right panel in Figure 2 contains a view of the geographic equatorial plane from above, and the left panel contains an illustration of the locations of the two spacecraft relative to the geomagnetic equator. Note that the field lines that pass through the two spacecraft do not

actually lie in the same plane, as shown in the left panel, but are drawn coplanar only to indicate the approximate geomagnetic latitudes of the two satellites.

The local-time separation in the GOES spacecraft has two effects. First, because GOES 9 lags GOES 8 in its orbit, it observes the spatial, diurnal variation in the particle flux with an offset corresponding to the separation in local time. Another important difference in the measured fluxes occurs because the spacecraft are located at different geomagnetic latitudes. Although both spacecraft are located at the geographic equator, Earth's magnetic dipole is tilted toward the geomagnetic equator in approximately the longitude of GOES 8. As a result of the dipole tilt, GOES 8 is at a geomagnetic latitude of about 11°. The dipole tilt has a much smaller effect on the geomagnetic latitude of GOES-9, which is about 4°. Although GOES 8 and 9 are both located at the geographic equator, GOES 8 is at a higher geomagnetic latitude and, therefore, under most circumstances will be measuring particles in larger L shells.

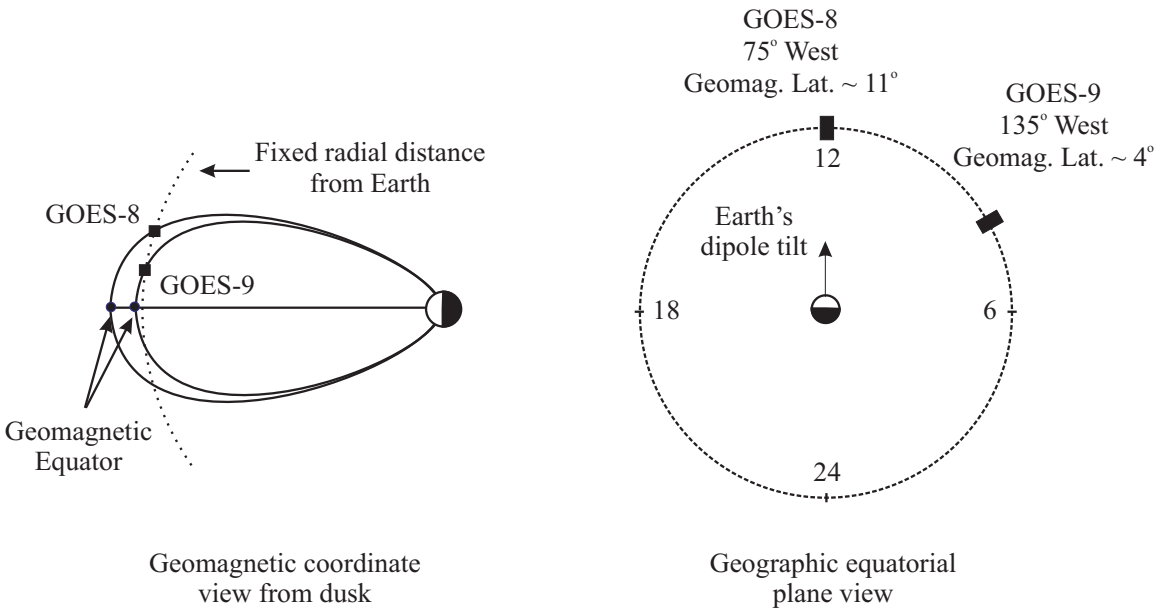

Figure 2. The geomagnetic latitudes of GOES 8 and GOES 9 (left) and their locations in the geographic equatorial plane (right). Note that although the east and west GOES satellites are both located in the geographic equatorial plane, the tilt of Earth's dipole results in a geomagnetic latitude difference of about 7°.

In order to establish that the electron detectors are accurately inter-calibrated and that the flux difference is in fact due to the longitudinal separation of the spacecraft, we have analyzed data from time intervals when GOES 9 was located close to GOES 8, prior to arriving at it operational location. Shortly after launch in May 1995, GOES 9 was located at about 90° west Longitude, about one hour in local time from GOES 8. It remained there until December 1995, when it was moved to 135° west Longitude.

A comparison of flux measurements from these times with different longitudinal separations is shown in Figure 3. This figure contains scatter-plots of the >2 MeV integral flux measured at GOES 8 versus the flux measured at GOES 9. The measurements in Figure 3a are from the three-

day period from Feb. 3-6, 1996 (from the middle of the interval shown in Figure 1). The GOES 9 measurements have been shifted four hours later in time so that each point represents the flux measured at the same local time by the two spacecraft. Some scatter occurs due to the temporal variations in the flux over the four hours between the GOES 8 and 9 measurements.

It is clear in Figure 3a that there is an offset in the measurements, with GOES 9 (at a lower geomagnetic latitude) measuring higher fluxes than GOES 8. This is consistent with the fact that at constant energy, radiation belt flux in the vicinity of geostationary orbit decreases with increasing radial distance from Earth.

Measurements made when the two spacecraft were at nearly equal geomagnetic latitudes are shown in Figure 3b. These data were obtained over the three-day period from July 3-5, 1995,

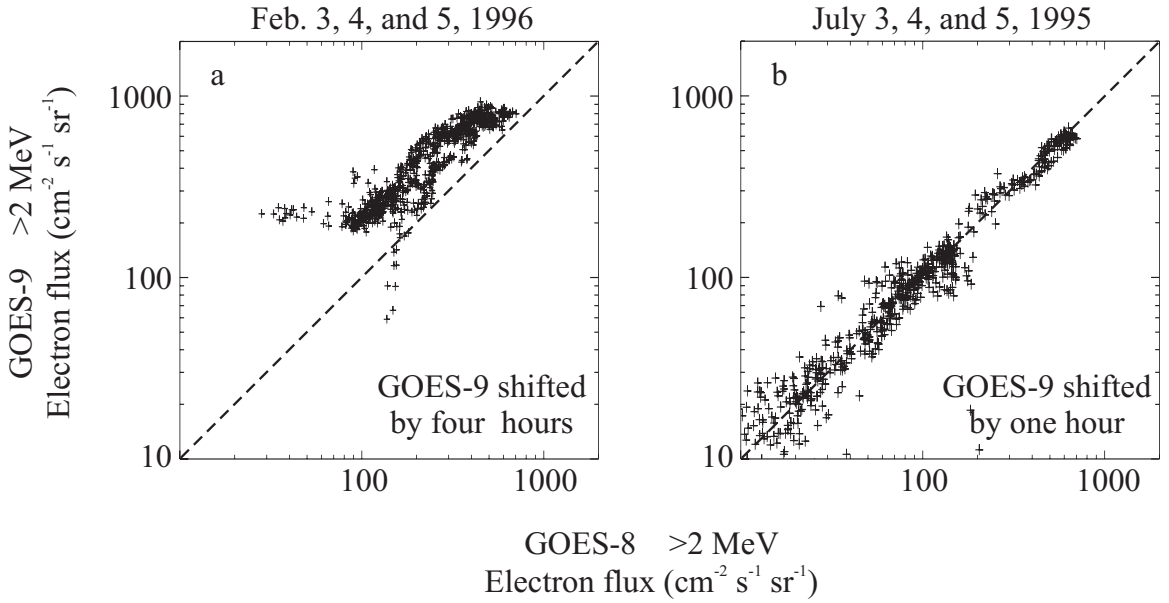

Figure 3. (Left) comparison of GOES 8 and 9 measurements obtained when the spacecraft were separated by four hours of local time and roughly 7° in geomagnetic latitude, and (right) when the spacecraft were separated by only one hour of local time and at approximately equal geomagnetic latitudes.

when GOES 9 was located one hour to the west of GOES 8. At this longitude, the geomagnetic latitude of GOES 9 was about 10.5°, within about 0.5° of the latitude of GOES 8. For this plot, the GOES 9 data were shifted in time by one hour, so that the values represent the flux measured at the same local time.

The close agreement between the GOES 8 and 9 measurements when the two spacecraft were at nearly equal geomagnetic latitudes indicates that the electron detectors are well inter-calibrated, and that the systematic difference seen in Figure 3a is due mainly to the geomagnetic latitude difference. Another factor that could contribute to the difference in flux measured at GOES 8 and 9 is the slightly different inclination of the magnetic field at the two spacecraft and any anisotropy in the pitch angle distributions. This, however, is not likely to cause a large effect,

given the broad field of view of the detectors and their westward look direction. Since the magnetic field inclination at geostationary orbit is primarily either toward or away from Earth, the westward-pointing detectors will always measure a broad range of pitch angles including 90°, even in the extreme cases of purely vertical or purely horizontal fields.

The GOES satellites, with their well inter-calibrated detectors and their simultaneous measurements in slightly separated *L*-shells, provide measurements that can be used to estimate the radial gradient of phase space density. The radial gradient, or $\partial f/\partial L$, is estimated by calculating phase space density at fixed values of the first two adiabatic invariants, *M* and *K*, and then comparing these values at different locations in *L*.

Two main assumptions are made to allow the calculation of phase space density at fixed *M* and *K* from the measured integral fluxes at fixed energies. The first assumption is that electron phase space density can be approximated with an exponential distribution:

$$f(E) = f_o e^{-E/E_o} \qquad (1)$$

which is related to the differential directional number flux, *j(E)*, and the particle momentum, p, by:

$$f(E) = \frac{j(E)}{p^2}. \qquad (2)$$

The integral flux is related to the differential flux by

$$J(>E) = \int_E^\infty dE'\, j(E') \qquad (3)$$

or,

$$J(>E) = \int_E^\infty dE'\, f(E')p^2 . \qquad (4)$$

With the assumed functional form of phase space density, (1), we can integrate (4) directly and solve for *f(E)* in terms of the measured integral flux, *J(>E)*,

$$f(E) = \frac{c^2 J(>E)}{(E_0{}^2 + EE_0)2mc^2 + 2E_0^3 + 2EE_0^2 + E^2E_0}. \qquad (5)$$

The second main assumption used in this analysis is that the pitch angle distribution at the equator can be described by:

$$f_{eq}(E, \alpha_{eq}) = f_{eq}(E)\sin^m \alpha_{eq}. \qquad (6)$$

The phase space density at a given pitch angle and energy at any latitude, λ, along a field line is equal to the phase space density at the same energy and its corresponding pitch angle at the equator (from Liouville's Theorem):

$$f_\lambda(E,\alpha_\lambda) = f_\lambda(E)g(\alpha_\lambda) = f_{eq}(E,\alpha_{eq}) = f_{eq}(E)\sin^m\alpha_{eq}\,. \qquad (7)$$

From conservation of the first adiabatic invariant, M,

$$M = \frac{p_\perp^2}{2mB} = \frac{p^2\sin^2\alpha}{2mB}, \qquad (8)$$

$$\sin\alpha_{eq} = \left(\frac{B_{eq}}{B_\lambda}\right)^{\frac{1}{2}}\sin\alpha_\lambda\,, \qquad (9)$$

so that,

$$f_\lambda(E,\alpha_\lambda) = f_\lambda(E)\sin^m\alpha_\lambda = f_{eq}(E)\left(\frac{B_{eq}}{B_\lambda}\right)^{\frac{m}{2}}\sin^m\alpha_\lambda\,. \qquad (10)$$

Therefore, the pitch angle dependence will have the same functional form everywhere along the field line. The peak amplitude of the phase space density (at 90° pitch angle) at latitude λ on the field line will be related to the peak amplitude at the equator by:

$$f_\lambda(E) = f_{eq}(E)\left(\frac{B_{eq}}{B_\lambda}\right)^{\frac{m}{2}}. \qquad (11)$$

Combining (5) and (11), we obtain the phase space density at 90° pitch angle at the magnetic equator as a function of the measured integral flux at latitude λ at 90° pitch angle,

$$f_{eq}(E) = \frac{c^2 J_\lambda(>E)}{({E_0}^2 + EE_0)2mc^2 + 2E_0^3 + 2EE_0^2 + E^2E_0}\left(\frac{B_{eq}}{B_\lambda}\right)^{\frac{m}{2}}. \qquad (12)$$

Using (12), phase space density is calculated for equatorially mirroring particles ($K = 0$), with magnetic moment $M = 6000$ MeV/G. A magnetic moment of 6000 MeV/G corresponds roughly to 2 MeV electrons in a 100 nT magnetic field, which is a typical field strength at geosynchronous orbit. The phase space density is first determined for 2 MeV particles from the measured integral flux, and then calculated for the appropriate energy for the selected value of M using (1).

A magnetic field model is used to calculate the ratio of the local and equatorial fields used in (12) and the L^* parameter [Roederer, 1970], which is related to the third adiabatic invariant,

$$L = L^* = \frac{2\pi k_0}{a\Phi}, \qquad (13)$$

where k_0 is Earth's magnetic dipole moment, a is the radius of Earth, and Φ is the magnetic flux enclosed in the particle drift. For this example, we have done the calculations using the Tsyganenko 1989 and the Tsyganenko 2001 and verified that for these quiet conditions, our results do not depend on this choice of field model.

The results of the *L*-shell calculations for the two spacecraft and the energy of the particles corresponding to M = 6000 MeV/G are shown in Figure 4. The upper panel (a) contains the measured >2 MeV electron flux, which is also shown in Figure 1. Panel (b) contains the calculated *L* values, and panel (c) contains the particle energies, which vary to maintain constant magnetic moment as the magnetic field varies. In panels (a)-(c), the GOES 8 values are shown with a solid line and the GOES 9 values with a dashed line. As seen in panel (c), the choice of M = 6000 MeV/G insures that the energies used in our analysis are near the measured energy, which minimized the dependence of our results on E_0 (through Equation (1)). Panel (d) contains the difference in the *L* values at the two spacecraft, $\Delta L = L_9 - L_8$.

Note that although GOES 8 is always at a higher geomagnetic latitude than GOES 9, GOES 8 is sometimes at lower *L*-shells. This is due to the asymmetric magnetic field, which is more compressed (resulting in lower *L*-shells) near noon than near midnight.

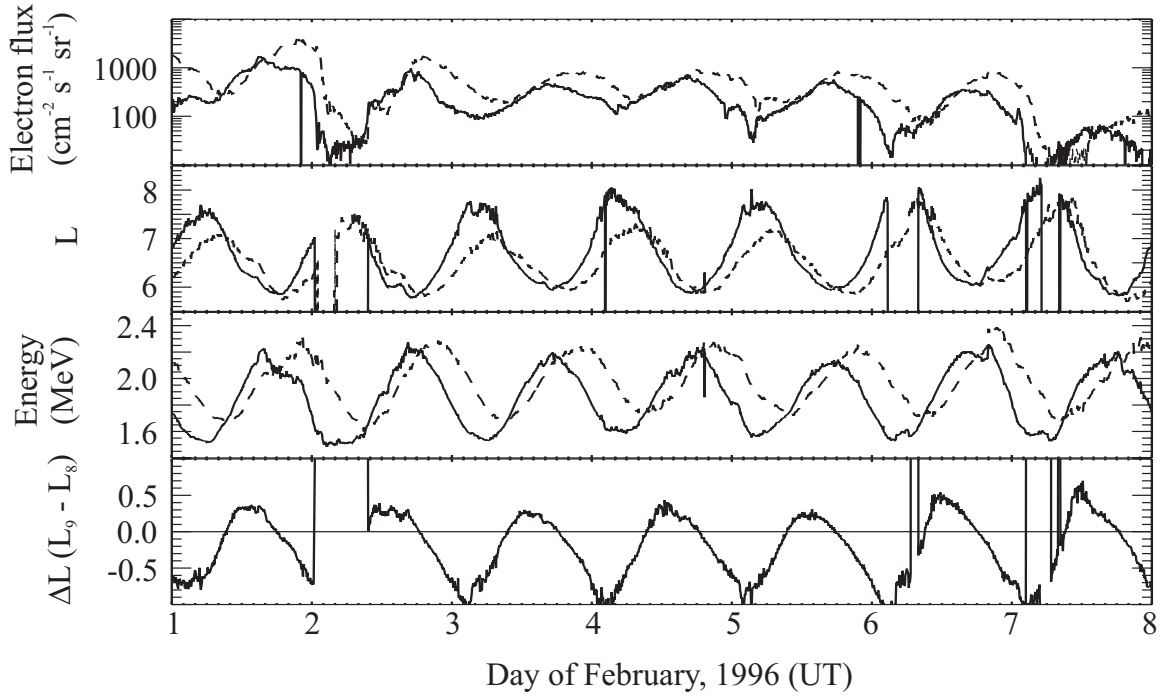

Figure 4. Electron flux, *L*-shell, particle energy for constant magnetic moment, and the *L*-shell difference of the GOES 8 and 9 measurements. Note that twice per day the two spacecraft are simultaneously measuring electrons in the same L-shell.

Consequently in the dawn magnetosphere, the increased compression in the magnetic field experienced by GOES 8 relative to GOES 9 as GOES 8 leads in local time by four hours causes the GOES 8 *L*-shells in this region to be lower than those of GOES 9. There are two *L*-shell crossings each day, one post midnight and one near noon, which correspond to times when the two spacecraft are simultaneously in the same *L*-shell.

These measurements made by the two satellites in the same *L*-shell give us the opportunity to test our assumptions about the particle distributions and to investigate uncertainties in the magnetic field models. As outlined above, the two parameters that need to be estimated to calculate phase space density from the measured integral fluxs are the index, m, in the pitch angle distribution (10) and the characteristic energy, E_0, in the energy distribution (1). The pitch angle index is estimated by considering the measurements at the locations where the two spacecraft are simultaneously in the same *L*-shell. At these locations, the calculated phase space density should be equal.

For the example presented here, we have only considered equatorially mirroring electrons (K= 0). Therefore, the calculations of L depend only on the equatorial magnetic field strength. Times when the L values for the two spacecraft are equal correspond to times when the equatorial magnetic field strengths are equal. At these times, the energies of the particles being considered are also equal, for a fixed magnetic moment. The ratio of the phase space densities at these locations reduces to:

$$\frac{f_8(E)}{f_9(E)} = \frac{J_8(>2)}{J_9(>2)}\left(\frac{B_{8\lambda}}{B_{9\lambda}}\right)^{\frac{m}{2}} = 1. \qquad (14)$$

Therefore, from the measured integral flux and the model magnetic field, (14) can be used to estimate the pitch angle index in the vicinity of the *L*-shell crossings.

Calculations of phase space density in the vicinity of the *L*-shell crossing ($\Delta L = 0$) that occurred at 0930 UT on February 4 are shown in Figure 5. The left panel illustrates the dependence of the difference in phase space density measured at the two spacecraft, $\Delta f = f_9 - f_8$, on the assumed value of m. This analysis indicates that phase space density is equal at the *L*-shell crossing when a weak pitch angle dependence ($m \sim 0.25$) is assumed. At this time (0930 UT), GOES 8 was located at 0430 LT and GOES 9 was located at 0030 LT. This result is reasonable, given that the electron distributions can range from being highly peaked at 90˚ near local noon (large values of m) to having a local minimum at 90˚ near midnight [e.g., West et al., 1973a,b; Selesnick and Blake, 2002].

Calculations of the difference in phase space density measured at the two spacecraft, $\Delta f = f_9 - f_8$, versus the difference in L-shells, $\Delta L = L_9 - L_8$ in the vicinity of this *L*-shell crossing are shown in the middle panel Figure 5. These results are from the time interval 0800 – 1100 UT, a three-hour interval centered on the *L* -shell crossing. The values of Δf and ΔL shown in Figure 5 indicate that phase space density had a positive radial gradient ($\partial f/\partial L > 0$) at this time. On either side of the *L*-shell crossing, the spacecraft at the large L measured a larger phase space density. The magnitude of $\partial f/\partial L$ is estimated by the slope of the least-squares fit to the calculations. For

E_0 = 250 keV (used for the calculations shown in the middle panel), the slope is approximately 1.3, corresponding to $\partial f/\partial L \sim 1.3 \times 10^{23}$ (MeV s L)$^{-1}$. The dependence of $\partial f/\partial L$ on the characteristic energy, E_0, is shown in the right panel of Figure 5. It is found that the value of $\partial f/\partial L$ is maximum and positive for low values of E_0, and decreases as E_0 increases. Over the full range of expected E_0 values [e.g., Cayton et al., 1989; McAdams et al., 2001], $\partial f/\partial L$ remains positive in the vicinity of this L-shell crossing.

A similar analysis has been performed for the L-shell crossing that occurred near local noon, at about 18 UT on February 4 (not shown). Near local noon, the pitch angle index required to have equal values of phase space density at the calculated L-shell crossing was $m \sim 12$. Although this value of m is quite large, it is consistent with observations of pitch angle distributions that are strongly peaked at 90˚ near local noon [e.g., Selesnick and Blake, 2002]. We have independently inspected pitch angle distribution using Polar data near noon and found examples where this value of m is reasonable. The calculated slope of the Δf versus ΔL values shows a positive radial gradient of phase space density, consistent with the results obtained from the earlier L-shell crossing.

The results presented here demonstrate that the well inter-calibrated electron detectors on the GOES satellites can be used to calculate the local radial gradient of phase space density at geosynchronous orbit due their separation in geomagnetic latitude. This example also indicates

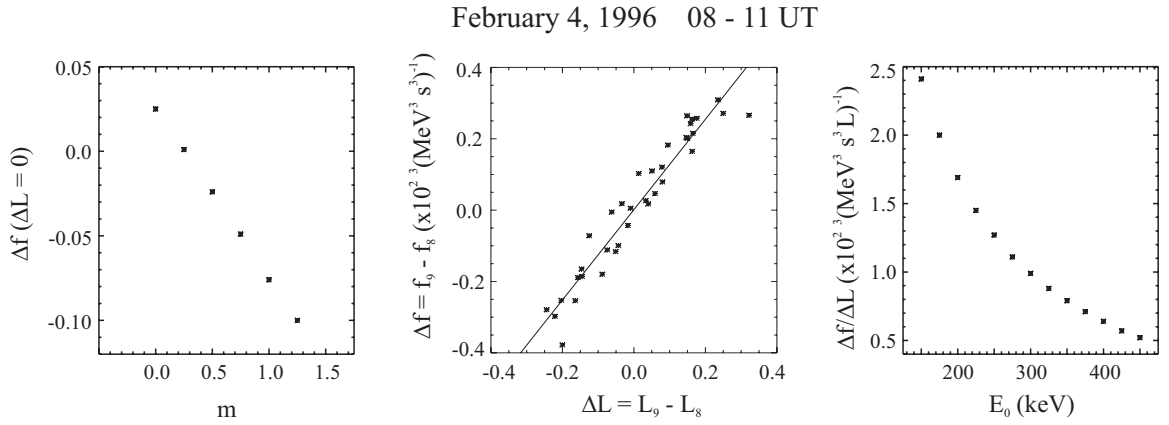

Figure 5: (Left) dependence of the value of df at the night-side L-shell crossing, (middle) phase space density difference versus separation in L-shell in the vicinity of the L-shell crossing, and (right) dependence of $\partial f/\partial L$ on the assumed value of E_0.

the importance of the pitch angle distribution in the calculations, and our ability to use the times when the spacecraft are simultaneously located in the same L-shell (based on the model magnetic field) to estimate the index of the pitch angle distribution (independent of the characteristic energy of the distribution function). Following the research plan described below, this technique will be further tested and applied to years of geosynchronous measurements, utilizing simultaneous pitch angle measurements from spinning GOES satellites (described below), and using additional data for the LANL geosynchronous satellites and from the Polar satellite during selected times to further constrain the global magnetic field model, the energy spectra, and the pitch angle distributions.

Research Plan

This research will be conducted over a three-year period and will quantify the phase space density of radiation belt electrons and its radial gradient at geostationary orbit. These results will establish a reference for the direction of radial diffusion and the variability of phase space density under a wide range of solar wind and geomagnetic activity conditions.

Our first task will be to calculate phase space density and its radial gradient over long time periods, including quiet and active conditions, using pitch angle measurement obtained from a third GOES satellite when one was in on-orbit storage and spinning. Over nearly two years from August 1998 to May 2000, GOES 9 was spinning and acquiring data at approximately 100º west Longitude, between GOES 8 and GOES 10 at the east and west operational locations (75º west and 135º west, respectively). For about one year from December 2001 until January 2003, GOES 12 was spinning and acquiring data at approximately 90º west Longitude, and GOES 11 began transmitting data while spinning in July 2003 and will continue to transmit data as long as GOES 12 (east) and GOES 10 (west) remain operational. These data are available with up to 10.24-second resolution. The first calculations will be done for a single magnetic moment, $M = 6000$ MeV/G, and for equatorially mirroring particles, $K = 0$. We will initially use the Tsyganenko 1989 field model, which can be parameterized with the Kp index only. We will then compare our results using other magnetic field models, such as Tsyganenko 2001, to investigate the dependence of our results on the field model.

Over these time periods, which include the approach to solar maximum and now the declining phase of Solar Cycle 23, pitch angle measurements were made continuously by the spinning spacecraft. We will use the simultaneously measured pitch angle distributions to calculate phase space density and its radial gradient using the technique described above. With these long periods of pitch angle measurements, we will characterize statistically the functional forms of the pitch angle distributions as a function of local time, geomagnetic activity, and local magnetic field inclination. Assuming a consistent statistical relationship for pitch angle distributions emerges, this result can be applied to the full GOES data set, including those time for which direct pitch angle measurements are not available.

In the example described above, the pitch angle index was determined at the *L*-shell crossings under the assumption that the magnetic field model was correct. During the extended times when pitch angle measurements are available, we will be able to use the measured pitch angle distributions to investigate the accuracy of various magnetic field models in determining the locations of the *L*-shell crossings. This will provide an additional consistency check on our results, which will be particularly valuable during active times when the magnetic field may be changing rapidly.

Our second task will be to use Polar and LANL geosynchronous data to further refine and validate our calculations during selected time intervals of interest. The Polar spacecraft made a large number of equatorial crossings near geosynchronous orbit, covering nearly all local times (see Figure 6 of Selesnick and Blake [2002]). These crossings provide electron energy spectra, electron pitch angle, and magnetic field measurements that can be compared with the GOES

measurements and with the magnetic field model. The LANL data will provide dense coverage at geosynchronous orbit of the electron energy spectra, magnetic field inclination, and pitch angle distributions, using techniques recently developed for identifying preferred directions in the electron flux measurements. These measurements will be used to validate, and if necessary, to modify our specifications of the electron distributions used in our calculations. In addition, the magnetic field measurements from GOES and Polar and the determination of the magnetic field inclination made by LANL will provide strong constraints on the magnetic field model used for our calculations of the adiabatic invariants. We are particularly interested in determining if the most recent magnetic field model by K. Tsyganenko, which includes azimuthally asymmetric fields in the magnetosphere, can be used to find an optimal fit to our multi-point determination of the magnetic field and phase space density.

Our third task will be to extend our calculations of adiabatic invariants to include off-equatorially mirroring particles. These calculations will be limited to time periods when we have sufficient confidence in the measured energy spectra, pitch angle distributions, and magnetic field model. We anticipate that we will utilize the most recent magnetic field model available, using the full constellation of satellites to determine the optimal model inputs. From our investigations of the pitch angle distributions, energy distributions, and sensitivity of the phase space density calculations on these parameters and on the parameterized magnetic field, we will know the level of confidence we can have in processing the GOES data over a full solar cycle (1995 – 2006), which would include the time periods for which we do not have simultaneous GOES pitch angle measurements. If the electron distributions can be parameterized sufficiently accurately by geomagnetic activity or magnetic field inclination, then this extension of our processing of the data will yield a full solar cycle of radiation belt electron phase space density mapped to adiabatic invariant space.

In addition to publications of our research, this effort will result in a number of deliverables to the LWS program. First, the dataset of phase space density mapped to adiabatic invariant space will be made available, together with the raw satellite measurements. And second, the source code used to calculate the adiabatic invariants will be made available with sufficient documentation that researchers will be able to reproduce and to extend our results. We feel it is critical for the progress of radiation belt research that measurements mapped to adiabatic invariant space and the tools needed to perform this mapping are made broadly available. Our documented source code will allow researchers to calculate the adiabatic invariants, M, K, and L^*, with the magnetic field models that we will use (T89, T2001, and others that include azimuthal asymmetry) and will give people the flexibility to modify and recompile the source code and take advantage of other magnetic field models as they desire.

At the end of this research, we will have determined the variability of phase space density and its radial gradient at geosynchronous orbit in terms of the adiabatic invariants over a minimum of many years, including the approach to solar maximum, near solar maximum, and now during the declining phase of Solar Cycle 23, and perhaps over the full solar cycle. This research includes the development and application of a new technique for calculating the radial gradient of phase space density, which exploits the separation in L-shell of longitudinally separated geostationary satellites. From years of direct pitch angle measurements made by

spinning GOES satellites, we will characterize the pitch angle distributions as functions of local time and geomagnetic activity.

The results of this research will provide critical new information for determining the source and loss processes operating in the radiation belts. In addition, our calculated values of phase space density in adiabatic-invariant space and the source code used to make these calculations will be made available through LWS-supported data and model centers for other researchers to use and extend. This effort contributes directly one of the specific research topics of high current interest in the TR&T program (the generation and decay of the Earth's radiation belts as a function of geomagnetic and solar wind conditions), and is relevant to four of the five NASA Strategic Enterprises. This research will improve our understanding of the basic response of magnetospheric electrons to solar variability and internal source and loss processes, and provide valuable information for the planning of future Living With a Star missions, such as the Radiation Belt Storm Probes, and the interpretation of their data.

Data Availability

For this research we will utilize data from the NOAA and LANL geosynchronous satellites, the ISTP Wind, and ACE satellites. Beginning early 1995, nearly continuous solar wind data are available from Wind and later from ACE. Periodic data outages during times such Wind perigee passes are not critical for this analysis. These data are available through CDAWeb and the NSSDC, and the real-time quick-look ACE data are available at NOAA/SEC.

Continuous geosynchronous energetic particle and magnetic field measurements are available from the NOAA GOES spacecraft: GOES-8 (launched May, 1994 and currently operating), GOES-9 (launched May, 1995 and removed from operation in 1998), and GOES –10 (launched in April, 1997 and currently operating). These data are all readily available at NOAA SEC. Energetic particle data are available from up to four simultaneously operating LANL spacecraft over the time period from 1995 to the present and these data are readily available at LANL. Data from the Polar spacecraft are available through Aerospace Corp. (see attached letter).

Project Management and Schedule

The Principal Investigator, T. Onsager, will have overall responsibility for establishing goals and milestones for this research. T. Onsager will be responsible for processing the NOAA data, including calculations of the pitch angle distributions and phase space density. J. Green and S. Elkington will be responsible for calculating the adiabatic invariants using their current software and for extending this software to allow the calculation of adiabatic invariants for off-equatorially mirroring particles. They will also provide the code documentation for when the software is delivered to the LWS program. J. Green will be responsible for processing the Polar data. G. Reeves will be responsible for collecting and verifying the LANL data, and providing magnetic field inclination and pitch angle distributions. All investigators will collaboratively conduct the research tasks described above. In addition, Dr. Anthony Chan of Rice University, who has been involved in the initial calculations of phase space density described here, will also participate as an unfunded collaborator (see attached letter). Although the order of the tasks may

vary slightly as the research develops, it is anticipated that the first tasks will be accomplished during Year 1 of this effort, the second task will be accomplished during Year 2, and the third task will be accomplished during Year 3.

Facilities and Equipment

All required facilities and equipment to conduct this research are currently available at the NOAA Space Environment Center, University of Colorado, Boulder, and at Los Alamos National Laboratory.

References

1. Brautigam, D. H., and J. M. Albert, Radial diffusion analysis of outer radiation belt electrons during the October 9, 1990 magnetic storm, J. Geophys. Res., 105, 291, 2000.

2. Elkington, S. R., M. K Hudson, and A. A. Chan, Resonant acceleration and diffusion of outer zone electrons in an asymmetric geomagnetic field, J. Geophys. Res., 108, 1116, doi:10.1029/2001JA009202, 2003.

3. Friedel, R. H. W., G. D. Reeves, and T. Obara, Relativistic Electron Dynamics in the Inner Magnetosphere - a Review, JASTP, (64) 265-282, 2002.

4. Hilmer, R. V., and G. P. Ginet, Enhancement of equatorial energetic electron fluxes near L=4.2 as a result of high speed solar wind streams, J. Geophys. Res., 105, 23,311, 2000.

5. Horne, R. B., and R. M. Thorne, Potential waves for relativistic electron scattering and stochastic acceleration during magnetic storms, Geophys. Res. Lett., 25, 3011, 1998.

6. Kim, H.-J., and A. A. Chan, Fully adiabatic changes in storm-time relativistic electron fluxes, J. Geophys. Res., 102, 22,107, 1997.

7. Li, X., D. N. Baker, M. Temerin, T. E. Cayton, G. D. Reeves, R. A. Christensen, J. B. Blake, M. D. Looper, R. Nakamura, and S. G. Kanekal, Multisatellite observations of the outer zone electron variation during the November 3-4, 1993 magnetic storm, J. Geophys. Res., 102, 14,123, 1997.

8. McAdams, K. L., G. D. Reeves, R. H. W. Friedel, T. E. Cayton, Multisatellite comparisons of the radiation belt response to the Geospace Environment Modeling (GEM) magnetic storms, J. Geophys. Res., 106, 10,869, 2001.

9. Roederer, J. G., Dynamics of Geomagnetically Trapped Radiation, 166 pp., Springer-Verlag, New York, 1970.

10. Selesnick, R. S., and J. B. Blake, A quiescent state of 3 to 8 MeV radiation belt electrons, Geophys. Res. Lett., 24, 1343, 1997a.

11. Selesnick, R. S., and J. B. Blake, Dynamics of the outer radiation belt, Geophys. Res. Lett., 24, 1347, 1997b.

12. Selesnick, R. S., and J. B. Blake, Radiation belt electron observations following the January 1997 magnetic cloud event, Geophys. Res. Lett., 25, 2553, 1998.

13. Selesnick, R. S., and J. B. Blake, On the source location of radiation belt relativistic electrons, J. Geophys. Res., 105, 2607, 2000.

14. West, H. I. Jr., R. M. Buck, and J. R. Walton, Electron pitch angle distributions throughout the magnetosphere as observed on Ogo 5, J. Geophys. Res., 78, 1064, 1973a.

15. West, H. I. Jr., R. M. Buck, and J. R. Walton, Satellite studies of magnetospheric substorms on August 15, 1968, 6, Ogo 5 energetic electron observations – Pitch angle distributions in the nighttime magnetosphere, J. Geophys. Res., 78, 3093, 1973b.